



Band-gap tuning of $\text{Cu}_2\text{ZnSn}(\text{S},\text{Se})_4$ solar cell absorbers via defined incorporation of sulphur based on a post-sulphurization process

Markus Neuwirth^{a,*}, Elisabeth Seydel^a, Jasmin Seeger^a, Alexander Welle^{b,c}, Heinz Kalt^a, Michael Hetterich^d

^a Institute of Applied Physics, Karlsruhe Institute of Technology (KIT), 76131 Karlsruhe, Germany

^b Institute of Functional Interfaces, Karlsruhe Institute of Technology (KIT), 76344 Eggenstein-Leopoldshafen, Germany

^c Karlsruhe Nano Micro Facility, Karlsruhe Institute of Technology (KIT), 76344 Eggenstein-Leopoldshafen, Germany

^d Light Technology Institute, Karlsruhe Institute of Technology (KIT), 76131 Karlsruhe, Germany



ARTICLE INFO

Keywords:

Kesterite

CZTSSe

Band-gap engineering

Chalcogenide ratio

Thin-film solar cells

Bandgap

ABSTRACT

We demonstrate that based on a post-sulphurization approach the mean sulphur concentration and bandgap of $\text{Cu}_2\text{ZnSn}(\text{S},\text{Se})_4$ (CZTSSe) solar cell absorber layers can be precisely controlled. However, X-ray diffraction and secondary ion mass spectrometry studies reveal an inhomogeneous sulphur incorporation at lower process temperatures resulting in a sulphur gradient in the absorber. Optimization of such gradients may enable further performance improvement of future devices. During the post-sulphurization process sulphur seems to accumulate at the back of the absorber first where there is already an enrichment of sulphur in the purely selenized absorbers. With higher temperatures more sulphur gets incorporated and the sulphur distribution gets evened out. Morphology studies show that the process of exchanging the chalcogenides leaves behind holes and results in a porous absorber layer. With higher process temperatures and therefore higher sulphur content the absorber gets more dense. The device performance of the post-sulphurized samples increases significantly with increasing process temperature and increasing sulphur content.

1. Introduction

Kesterite $\text{Cu}_2\text{ZnSn}(\text{S},\text{Se})_4$ (CZTSSe) is among the most promising materials in photovoltaics in the last years [1–4] not only for its earth-abundant and non-toxic constituents, but also for its material properties. One very interesting and useful feature is the tunability of its bandgap. This can be achieved by either substituting Sn by Ge [5–9] or by changing the absorbers' chalcogenide ratio $[\text{S}]/([\text{S}] + [\text{Se}])$ [10–16]. Both result in a band-gap range of roughly 1.0 eV – 1.5 eV and can therefore be used to fit the bandgap best to the solar spectrum [17]. The current record cell with 12.6 % power conversion efficiency reported by Wang *et al.* for instance had a bandgap of 1.13 eV [18] due to a chalcogenide ratio >0 . Combining both Germanium incorporation and chalcogenide ratio modification offers the possibility of fabricating high bandgap kesterites that can be used as part of tandem solar cells [19].

Another potentially beneficial technique within band-gap engineering is band-gap grading as it is done in $\text{Cu}(\text{In},\text{Ga})\text{Se}_2$ (CIGSe) [20–23] and has also been investigated for kesterites [24–26]. Woo *et al.* realized CZTSSe solar cells with a gradually increasing bandgap from front to back of the absorber leading to an enhanced carrier

collection, a decrease in carrier recombination and therefore an enhancement of the short-circuit current [24]. With the different approach of front-surface band-gap grading Yang *et al.* were able to fabricate a device with 12.3 % efficiency due to an increased bandgap in the vicinity of the depletion region leading to significant improvements in the open-circuit voltage [26].

In this study we focus on the modification of the absorber's chalcogenide ratio to tune its bandgap. With our technique we are able to adjust the bandgap within the given range of 1.0 eV – 1.5 eV as we recently reported [27]. In this work we take a closer look at these samples concerning their morphology and elemental distribution relative to their chalcogenide ratio. A clear connection between the amount of sulphur in the absorber, its morphology and device performance, as well as clear trends for future process improvements and potential elemental gradients for band-gap grading will be shown.

* Corresponding author.

E-mail address: markus.neuwirth@kit.edu (M. Neuwirth).

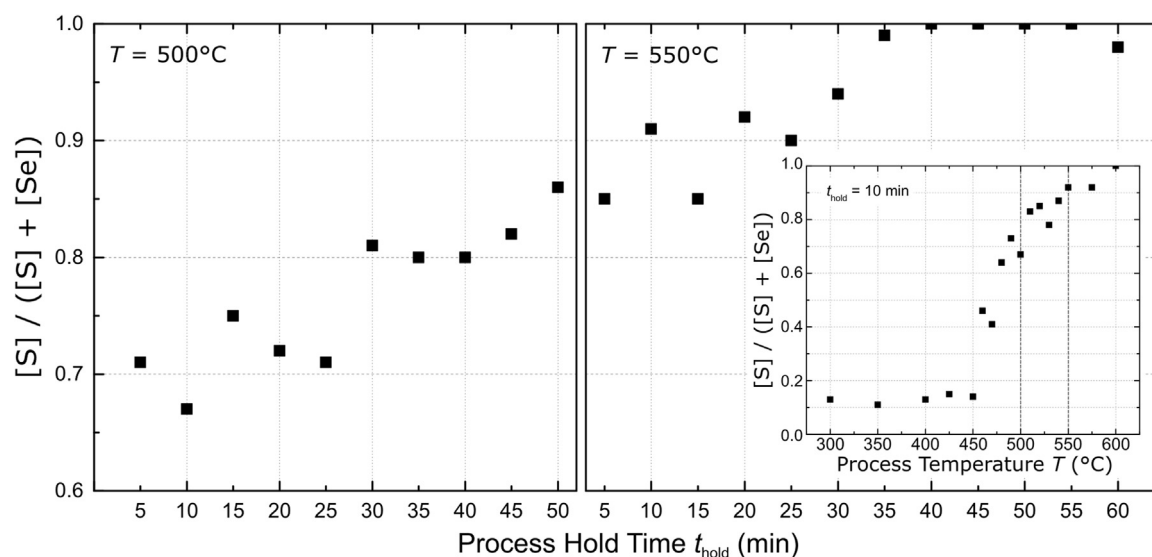


Fig. 1. Chalcogenide ratio $x = [S]/([S] + [Se])$ of several samples post-sulphurized at $T = 500^\circ\text{C}$ (left) and $T = 550^\circ\text{C}$ (right) plotted over the process hold time t_{hold} . t_{hold} is varied for both temperatures in steps of 5 min from 5 min to 50 min and 60 min, respectively. In the inset on the right x is plotted over the process temperature T for $t_{\text{hold}} = 10$ min. Both temperatures of the t_{hold} -series are marked by vertical lines. Data has already been shown at 44th IEEE PVSC in a similar fashion [27].

2. Material and methods

2.1. Fabrication

Fabrication of our absorber layers consists of two major parts. The first part is our already optimized process for selenium-rich absorber layers that is based on a wet-chemical approach [28,29]. We start with a metal-salt solution based on dimethyl sulfoxide. The solution contains copper acetate, zinc chloride, tin chloride and thiourea. It is applied onto a molybdenum-coated soda-lime glass via doctor-blading. The wet layer is then dried at 300°C under nitrogen atmosphere for 2 min. These steps are repeated six times to reach a precursor layer thickness of approximately $1\ \mu\text{m}$. This precursor is then annealed in a selenium-nitrogen atmosphere for 10 min at 540°C . The nitrogen background pressure is set to 250 mbar. This takes place in a home-made tube furnace whereby the sample and the selenium pellets are placed in a quasi-closed graphite box. The furnace is heated up using a ramp of $140^\circ\text{C}/\text{min}$. Afterwards the furnace is cooled down naturally. Due to the selenium-rich atmosphere this annealing step is called selenization. During selenization the sulphur in the precursor that was provided by the thiourea is almost completely replaced by selenium resulting in a chalcogenide ratio $[S]/([S] + [Se]) \approx 0.1$.

The idea is to adjust the sulphur content of the final absorber layer by modifying the fabrication process. However, we do not want to alter the existing selenization process in that manner for it being optimized and achieving satisfying results [29]. Thus we add an additional annealing step after the selenization to introduce sulphur into the already finished absorber. In this new post-sulphurization step the selenium-rich absorber is annealed in a sulphur-nitrogen atmosphere. Therefore, 500 mg of sulphur are added to the sample in the graphite box. Heating ramp and cool-down process do not differ from the selenization process. The nitrogen background pressure is set to 500 mbar. Process time and temperature are varied to adjust the final sulphur concentration.

All samples are broken in half after selenization with only one of the resulting pieces being post-sulphurized for having a purely selenized reference sample for each post-sulphurization experiment. Both halves are completed by a wet-chemically processed CdS buffer layer, a sputtered i-ZnO window layer and a sputtered ZnO:Al front-contact.

2.2. Characterization

The morphology of our samples was analyzed using a Carl-Zeiss-SUPRA-55VP scanning electron microscope (SEM) with 2 kV acceleration voltage. Every sample was measured by X-ray diffraction (XRD) to extract the position of the (112)-kesterite reflex for later evaluation of the sulphur-to-selenium ratio. A Bruker AXS D8 DISCOVER with a copper anode ($\lambda_{\text{Cu}} = 0.15406\ \text{nm}$) was used. The composition of the absorber layers was measured via energy-dispersive X-ray spectroscopy (EDX) using a Carl-Zeiss-LEO-1530 SEM with 10 keV acceleration voltage. Secondary-ion mass spectrometry (SIMS) measurements were conducted to analyze the samples regarding potential compositional gradients using a TOF.SIMS 5 from ION-TOF. Current-voltage characteristics were measured via a four-point probe measurement using a Keithley 2400 source measuring unit. The probes were placed directly on the ZnO:Al front contact. The measurements took place under simulated AM 1.5G solar irradiation by a Wacom Electronic WXS-155S-10 sun simulator (class AAA). The active area of the solar cells is approximately $0.16\ \text{cm}^2$. The series resistance R_s has been evaluated by a linear fit to the slope of the IV curve under illumination. The parallel resistance R_p has been extracted from the dark IV data using a curve fitting introduced by Gromov *et al.* [30].

3. Results and discussion

We prepared several CZTSSe absorber samples using different post-sulphurization temperatures T as well as different process hold times t_{hold} . — Before starting the discussion we like to note that even at high post-sulphurization temperatures no noticeable Sn-loss was observed. — We measured XRD diffractograms of all samples and analyzed the peak position of the (112)-kesterite reflex via a Gaussian fit. Knowing this position, the chalcogenide ratio $x = [S]/([S] + [Se])$ is calculated using Vegard's law. Parts of the results shown here (see Fig. 1) were already shown and discussed at the 44th IEEE PVSC [27]. This publication's aim is to further study these samples and deepen the knowledge about our post-sulphurization process. In Fig. 1, x is plotted over t_{hold} for two different process temperatures $T = 500^\circ\text{C}$ and $T = 550^\circ\text{C}$. An approximately linear dependency of x and t_{hold} is clearly visible covering $x \approx 0.7 - 1.0$, whereby the range of x for $T = 550^\circ\text{C}$ ties in seamlessly with its range at $T = 500^\circ\text{C}$. In the inset on the right the chalcogenide ratio x is plotted over the process temperature T for

Download English Version:

<https://daneshyari.com/en/article/6534128>

Download Persian Version:

<https://daneshyari.com/article/6534128>

[Daneshyari.com](https://daneshyari.com)